Follow your label: simultanous 4D angiography and perfusion imaging by arterial spin labeling MRI

Plas, M.C.E. van der

CHAPTER

SUMMARY AND GENERAL DISCUSSION

Summay

In the first chapter a general introduction of ASL was given. Different aspects that are important for the optimization of the ASL sequence for the acquisition of both angiography and perfusion images were discussed. Multiple approaches to acquire these two datasets simultaneously have been described and different k-space trajectories paired with their benefits were introduced.

The goal of the second chapter was to acquire a very high temporal resolution multi-timepoint ASL dataset while still maintaining whole brain coverage. The first source for the temporal resolution was a Hadamard preparation, for which the total labeling duration is divided into multiple sub-boli that are either label or control in accordance with a Hadamard matrix. During post-processing, the same matrix is used to decode which enables separation of the signal of each sub-boli. As a second source for the temporal resolution, a Look-Locker (LL) readout was used to achieve an higher temporal resolution by interpolating the timings of the Hadamard labeling blocks. For this readout, multiple low flip angle are performed after a single ASL preparation. This way, four images were acquired at an interval of 150 ms for every Hadamard line. By combining these two techniques, a temporal resolution of 75 ms up to a PLD of 1525 ms was obtained within this sequence. To provide whole brain coverage, the LL-readout was combined with a simultaneously multi-slice (SMS) readout to excite four slices simultaneously, which resulted in the acquisition of 16 slices within the short LL interval of 150 ms. This rich amount of data was then quantified using a more advanced kinetic model that isolates the macrovascular contribution to the ASL perfusion signal to prevent macrovascular contamination in the CBF maps. Since such a high temporal resolution dataset with 28 timepoints was acquired, it was investigated whether reducing the total scan time of 10 min would still give similar quality of the CBF maps. It was shown that even when the scan time is reduced to 1min18s, the ASL data would still provide good quality CBF maps.

Quantification of perfusion signal within ASL data can be overestimated, since the cerebral blood flow (CBF) maps can be contaminated with macrovascular signal. This could be the case if not all the labeled blood arrived at the tissue it will feed yet. Including a macrovascular component within the kinetic model to quantify the ASL signal, allows for the isolation and subsequent elimination of the macrovascular component. This alleviates the overestimation of the CBF since it separates the ASL signal into two components: a macrovascular and a tissue contribution. However, within this two-component kinetic model it is assumed that the well-

defined box-shaped bolus that is created at the labeling plane is preserved when it travles through the macrovasculature. Due to laminar flow profiles, bifurcations and bending of the vessel walls, the label will disperse. To obtain more realistic CBF estimations, a gamma dispersion kernel could be included in the kinetic model, which estimates and corrects for the dispersion of the labeled blood. It is not yet known how this correction will influence the CBF estimations, since it could potentially correct for the fact the some (trailing) spins did not arrive at the tissue yet which leads to higher CBF values. On the other hand, it could improve the separation of the macrovascular and tissue component which would lead to higher arterial blood volume (aBV) values and lower CBF values. In the third chapter, using the high temporal resolution data from chapter two, this is studied. A 4D ASL angiography dataset was acquired as a reference for the macrovascular component. It was shown that the inclusion of a gamma dispersion kernel within the kinetic model led to higher aBV values in all datasets; high (28 timepoints) and low (7 timepoints) temporal resolution ASL datasets and the 4D ASL angiography. For both the high and low temporal resolution ASL datasets this increase in aBV values was accompanied with a decrease in CBF values. Visual inspection led to the conclusion that arterial signals further down the arterial tree were correctly classified as macrovascular signal when a gamma dispersion kernel was included in the two-component kinetic model. Which suggests that the inclusion of a gamma dispersion kernel improves the isolation of the macrovascular signal from the perfusion signal. In addition the temporal resolution of the ASL data also influenced the separation between the two-components: within the lower temporal resolution ASL datasets, which were acquired without the LL-readout and thus provided 7 instead of 28 timepoints, less signal was identified as being of macroavascular origin compared to the high temporal resolution ASL dataset.

In the fourth chapter, the combination of a Hadamard ASL preparation with a golden angle radial readout was studied. A Hadamard preparation is able to provide multi-timepoint ASL data in a time efficient manner by dividing the total label duration in multiple sub-boli. The signal of each sub-boli is separated during postprocessing using the appropriate matrix for decoding. A golden angle radial readout provides the ability to obtain dynamic angiography and perfusion images from the same dataset. Radial sampling of k-space based on the golden angle principle allows for retrospective adaptation of the temporal resolution, since k-space is uniformly sampled for any arbitrary temporal window. Moreover, by focusing on the central portion of each spoke that is included in the reconstruction, the effective spatial resolution

can be adapted for perfusion imaging during the later timepoints. This readout therefore provides an extremely flexible approach to obtain multiple reconstructions form the same data, each with a different trade-off between spatial and temporal resolution. By combining these two techniques the SNR during the perfusion phase could be increase compared to the golden angle radial implementation of Okell. Moreover when using this k-space trajectory, the temporal resolution of the reconstructions can be chosen retrospectively which allows for the adaptation of the reconstructions to the specific hemodynamics of each subject that is scanned. This golden angle radial readout was combined with a Hadamard-8 matrix to increase SNR during the perfusion phase with a factor of 3.6 compared to previously proposed implementations of this readout that combined it with traditional pCASL. For a single slice implementation a minimal temporal resolution of 69 ms was achieved at a high spatial resolution of 0.78 x 0.78 x 12 mm^3. During the perfusion phase at a PLD of 1762 ms, only the densely sampled center of k-space was included in the reconstruction, which results in the desired lower spatial resolution perfusion images with adequate SNR. For multi-slice imaging, the Hadamard preparation was the only source for the temporal resolution, therefore the duration of the golden angle radial readout could be minimized, which allows for the acquisition of 10 slices after every Hadamard line. This way, angiographic and perfusion images were acquired in 10 consecutive slices, thereby depicting the passage of the labeled blood from the microvasculature towards the tissue with whole brain coverage.

Even though the combination of a Hadamard preparation with a golden angle radial readout is time-efficient and provided both angiography and perfusion data from a single scan, a radial sampling trajectory is not efficient with respect to the amount of k-space covered after each excitation pulse. Many radial spokes are needed to sufficiently cover k-space, and thus many excitation pulses are used during a radial readout causing significant attenuation of the labeled signal over the readout-period. A more efficient way of sampling k-space is a spiral trajectory. In the last chapter of this thesis, this trajectory was combined with a Hadamard-8 preparation. Since a 3D Stack of Spirals (SoS) was employed, high temporal resolution and high spatial resolution ASL-images were obtained for 4D MRA visualization, whereas low spatial resolution provided perfusion images. All acquired simultaneously within a single dataset, while maintaining whole brain coverage. The 4D MRA images are sparse which allows for undersampling of the outer part of k-space. Moreover, these MRA images already have a sufficient high SNR due to the fact that the labeled blood is concentrated within the

microvasculature and measured at short PLD. On the other hand, during the perfusion phase SNR should preferable be increased, which can be achieved by over sampling the center part of k-space. For this reason, three different datasets were acquired with each a different spiral trajectory: a uniform spiral and a variable density spiral with an undersampling factor of 2 and 3. Since the center of k-space was oversampled when using a variable density spiral, the SNR was increased during the perfusion phase. Alternatively, one can opt for reducing the total scan time by a factor of 2 when using the variable density dataset with an undersampling factor of 3.

Key findings

Time inefficiency

In itself, ASL is quite a time inefficient technique to obtain data, especially for perfusion imaging since longer PLDs are needed to allow the labeled spins to travel from the labeling region to the brain tissue that the blood is providing with oxygen and nutrients. Moreover, long labeling duration (typically around 2 seconds) are needed to label enough spins to allow detection above the noise level. In addition, to obtain adequate SNR within these perfusion images, ASL measurements are usually repeated around 30 times (either by pure averaging or by the readout of multiple segments in 3D sequences). These three aspects within an ASL sequence result in typical scan durations of 5 minutes for single-timepoint ASL datasets. For more accurate quantification of the ASL signal, multi time-point ASL is required. In addition both MRA and perfusion data are needed to get a detailed insight into the entire hemodynamic condition of the brain. Acquiring these ASL datasets sequentially is very time consuming and inefficient since both datasets can be acquired using the same ASL preparation. Therefore multiple methods have been investigated for the time efficient acquisition of multi-timepoint ASL datasets. Combining a Hadamard preparation with LL readout and SMS acquisition provided high temporal resolution multi-timepoint data with whole brain coverage within 10 minutes. This sequence resulted in 28 timepoints that provided detailed information about the entire hemodynamic status of the whole brain. It was also demonstrated in chapter two that lowering the scan duration to 1min18s, by eliminating multiple repeated measurements, still resulted in similar quality CBF maps compared to the 10 min scan. From this dataset the aBV and ATT maps were also estimated

which provided extra information about the hemodynamics of the brain and more accurate CBF estimations.

To be able to reconstruct both high spatial and high temporal resolution angiography and low spatial and low temporal resolution perfusion images from a single data set, a Hadamard matrix was combined with a golden angle radial readout. This readout allows for the retrospectively adjusting the temporal window based on the hemodynamics of the subject. A single-slice data set was acquired within 8 min and the angiographic phase was reconstructed at a temporal resolution of 69 ms. By focusing on the center part of the acquired radial spokes, perfusion signal was reconstructed at a low spatial resolution to enhance the SNR.

To enable whole brain coverage, while simultaneously acquiring 4D MRA and perfusion images, a 3D SoS readout was combined with a Hadamard preparation. The use of a variable density spiral, for which the outer part of k-space was undersampled and the center part of k-space oversampled, resulted in reduced scan times of a factor of two, resulting in a total scan time of less than 3 minutes. During these 3 minutes high temporal resolution and high spatial resolution 4D MRA and perfusion data was acquired. Moreover, since the center of k-space was oversampled, increased SNR was achieved for the perfusion phase of the ASL signal compared to when using a uniform spiral.

Quantification challenges

In the quantification process of ASL data, many assumptions are needed within the context of the kinetic model, which lead to uncertainties in the estimated CBF, ATT and aBV maps. For the standard processing of single time-point ASL datasets as stated in the 2015 consensus article, it is for example assumed that all the labeled blood has arrived in the tissue at the time of the readout. However, this is not always the case, which could lead to CBF maps that are contaminated with macrovascular signal at certain regions, whereas at other locations underestimation of perfusion signal occurs, because labeled spins did not arrive to that region. Both effects lead to local and global quantification errors. Acquisition of multi-timepoint ASL datasets could overcome this problem since two-component kinetic models could be fitted to this data which allow isolation of the macrovascular component from perfusion signal. In chapter three, one of the underlying assumptions of the was investigated: dispersion. Usually it is assumed that the well-defined box-shaped bolus that is created at the labeling plane is preserved when it traverses the macrovasculature. However, in reality this

box-shaped bolus will disperse, which is shown in figure 1. In chapter three, dispersion was taken into account when fitting the ASL data with a two-component kinetic model to study whether this would improve the separation of the macrovascular and perfusion signal. Inclusion of a gamma dispersion kernel led to increased aBV values and decreased CBF values. This indicates that when dispersion is taken into account, the kinetic model is better able to separate the macrovascular signal from the perfusion signal. Therefore, there will be almost no macrovascular contamination in the estimated CBF maps which will lead to more accurate CBF values.

Timing parameters in ASL sequence

In ASL timing parameters such as the label duration, temporal resolution and PLD in a sequence are important since they determine the type of image that is acquired. When scanning healthy volunteers these timings can be used from literature, such as described in the "white paper"[1]. However, when scanning patients in the clinic, these timings are more difficult to predict, since the arterial arrival time could be delayed in various degrees. When choosing all timing parameters a priori, and the patient does have an increased arterial arrival time, the angiographic signal will arrive at the imaging plane during the later PLDs. Usually these later PLDs signals are reconstructed with a low temporal and low spatial resolution as it is expected to be perfusion signal. This way the acquired data is not sufficient to make a diagnosis since the angiography is not reconstructed in an optimal way. To overcome this problem, the golden angle approach was adopted, which provides more freedom to adapt the temporal resolution and timing of MRI-sequence retrospectively. In Chapters four and five, a time-encoded ASL preparation was combined with non-Cartesian golden angle k-space trajectories. Filling k-space using a non-Cartesian golden angle sampling strategy allows for flexibility regarding both temporal and spatial resolutions, since k-space is always almost uniformly sampled for any arbitrary range of subsequent radial spokes or spirals. By including only the densely sampled center of k-space for the reconstruction, the spatial resolution can also be lowered, which is needed for perfusion imaging where label is more diluted and acquired after a longer waiting time in which the labeled signal has decayed considerably more compared to ASL-angiography. This way when a patient with delayed arterial arrival time is scanned, the angiographic signal can still be reconstructed at a high temporal and high

spatial resolution even when it arrives later at the imaging plane than expected, thereby still providing the relevant information as requested for the clinical diagnosis.

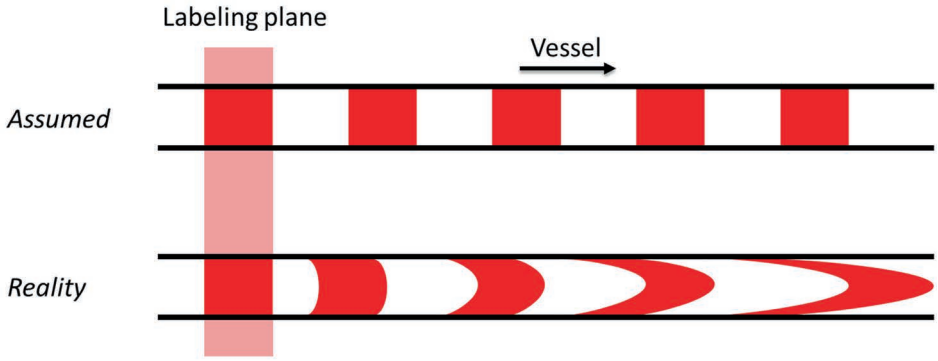

Figure 1. Dispersion. The top part shows how the well-defined box-shaped bolus that is created at the labeling plane is assumed to be preserved when is travels through the macrovasculature. The bottom part shows the reality which demonstrates that due to laminar flow profiles, bifurcations and bending of the vessel wall the labeling block will disperse.

ASL in the clinic and future aspects

In this thesis multiple advanced ASL sequences were developed and investigated for the simultaneous acquisition of angiographic and perfusion images. These high temporal, multi-timepoint ASL datasets were then used to improve the quantification of ASL signal and to obtain CBF, ATT and aBV maps. These quantitative maps hold the potential to provide important information in for example patients with stroke or Alzheimer's disease[2-5]. However, more research is needed to be able to apply these techniques within the radiological clinic.

Scan duration

The ASL sequences that were developed are very time-efficient since they can acquire both angiography and perfusion images simultaneously. However, for all the sequences that are described in chapter two, four and five the total scan time is around 10 min for either single slice, multi slice or 3D acquisitions. Due to this scan duration, these sequences are prone to motion artefacts and variabilities due to the cardiac and respiratory cycle. This could lead to data instability which results in quantification errors and a decrease in SNR. To overcome this,

the scan time should be further reduced and/or motion correction approaches should be included. Further scan time reductions could for example be achieved by using artificial intelligence (AI). It was recently shown by Lønning et al that MRI sequences can be strongly accelerated when using deep learning techniques[6]. Moreover, Yousefi et al demonstrated a 3D end-to-end convolutional neural network for the acceleration of te-pCASL data reconstructions[7].

Another approach to accelerate the ASL sequences and reduce the total scan time could be compressed sensing reconstructions. Zhao et al proposed a sparse model-based image reconstruction for a 3D multi-timepoint spiral ASL sequence[8]. They were able to reduce the scan time to 20 seconds for each timepoint by using a model-based sparsity constraint reconstruction while improving SNR. However, the low SNR during the perfusion phase makes it difficult to distinguish signal from noise. This led to the fact that a complex subtraction was used which could be less robust compared to a magnitude subtraction. This way, the compressed sense reconstruction was performed on the label and control images separately. This might make this approach more applicable to the angiography phase of the ASL signal, since during this phase a higher SNR is achieved.

Due to the complexity of the ASL sequences in this thesis, more advanced motion correction techniques were not applied, although their use could be highly beneficial. For example, the ASL sequence combining a Hadamard-8 matrix is with a LL and SMS readout as described in chapter two, would need to employ the motion correction technique proposed by Suzuki et al[9]. This technique can prevent severe background suppression subtraction errors after motion that arise due to the interleaved acquisition of the slices by means of SMS. Alternatively, 3D readout approaches can be used in which the background suppression is similar over the total imaging volume, thereby avoiding this specific type of motion artefacts. However, by using a segmented 3D approach, the total temporal footprint is increasing and motion correction between these segments might become necessary. In the ASL sequences in chapter four and five, non-Cartesian golden angle readouts were combined with a Hadamard labeling preparation. With these type of non-Cartesian golden angle approaches, the densely sampled center of k-space can also be exploited for motion correction when using more advanced reconstruction approaches such as iterative reconstructions[10, 11]. Or the affected radial spoke or spiral could be eliminated from the reconstruction to reduce motion artefacts.

3D trajectories

In this thesis the flexibility with respect to the temporal and spatial resolution within an ASL sequence was investigated using golden angle based non-Cartesian sampling strategies. This way both 4D MRA and perfusion images were acquired simultaneously within a single dataset. However, most of these acquisitions were single-slice or multi-slice, which limits the application within the clinic. In chapter 5 a first attempt was made to develop an ASL sequence with a non-Cartesian 3D readout. However, this was a stack-of-spiral 3D readout, i.e. a Cartesian sampling in the z-direction. To fully use the potential of non-Cartesian 3D readouts in combination with the flexibility in the temporal domain, a 3D golden angle spiral cone or a 3D golden angle radial kooshball would be of interest[12, 13]. With these non-Cartesian 3D acquisitions, the acquired radial spoke or spiral cone is always acquiring the center of k-space which allows for reconstruction with very limited data and allows to retrospectively choose the temporal resolution while still maintaining whole brain coverage.

Personalized ASL sequences

Creating more subject specific ASL sequences could also improve the applicability in the clinic. As stated in chapter two, having a rich amount of ASL data i.e. 28 timepoints and 16 slices, opens up new avenues. In the most simple approach visual inspection of a movie showing the inflow and distribution of labeled blood within the brain, provides the clinician with a much better impression of the individual hemodynamic status than a static perfusion image. Moreover, timing parameters maps harbor significant relevant information as for example exploited in acute stroke research, where timing parameters are frequently used for treatment selection. Limiting the amount of repeats within the sequence of Chapter 2, led to a scan time of little over 1 min without severe degradation of image quality of the estimated CBF maps, whereas the dynamic images could still provide insight into the arrival times of the labeled spins into the brain. This could also sever as a quick survey of the hemodynamic status of a patient, just as described by Dai et al., and as input for optimal setting for an ASL scan[14]. The non-Cartesian golden angle approaches of chapter four and five, also provide more subject specific sequences since the temporal resolution can be adapted retrospectively to the hemodynamics of the patients. Since in chapter four an online reconstruction was implemented, this will allow the lab technician to change the temporal and spatial resolution for a reconstruction immediately after the scan is acquired. Ideally, it would be of interest to

adapt these settings for the reconstruction automatically. However, this would requires AI approaches to be able to determine the temporal and spatial resolution automatically based on the hemodynamics of the subject. More research is necessary to investigate the full potential of these non-Cartesian golden angle approaches in combination with ASL and its application in the clinic.

Remaining quantification challenges

Next to the fact that ASL is a non-invasive technique, quantification of the ASL signal is another major advantage. However, the employed kinetic model is based on many assumptions and is prone to quantification errors due to uncertainties within these assumptions. In this thesis some of the aspects were investigated such as the influence of dispersion and the temporal resolution on the estimation of the macrovascular component in multi-timepoint ASL data. However, other uncertainties that could lead to quantification errors remain, such as uncertainties in label inefficiency, differences in T_1 of arterial blood and variation in ATT values[15].

Bibliography

1. D.C. Alsop, J.A. Detre, X. Golay*, et al.*, Recommended Implementation of Arterial Spin Labeled Perfusion MRI for Clinical Applications: A consensus of the ISMRM Perfusion Study Group and the European Consortium for ASL in Dementia*. Magnetic Resonance in Medicine,* 2015.
2. J.A. Chalela, D. Alsop, J.B. Gonzalez-Atavales*, et al.*, Magnetic Resonance Perfusion Imaging in Acute Ischemic Stroke Using Continuous Arterial Spin Labeling*. Stroke,* 2000. 31: p. 680-687.
3. J. Demeestere, A. Wouters, S. Christensen, R. Lemmens and M.G. Lansberg, Review of Perfusion Imaging in Acute Ischemic Stroke: From Time to Tissue*. Stroke,* 2020. 51(3): p. 1017-1024.
4. N. Zhang, M.L. Gordon and T.E. Goldberg, Cerebral blood flow measured by arterial spin labeling MRI at resting state in normal aging and Alzheimer's disease*. Neurosci Biobehav Rev,* 2017. 72: p. 168-175.
5. C.E. Wierenga, C.C. Hays and Z.Z. Zlatar, Cerebral blood flow measured by arterial spin labeling MRI as a preclinical marker of Alzheimer's disease*. J Alzheimers Dis,* 2014. 42 Suppl 4: p. S411-9.
6. K. Lønning, P. Putzky, J.-J. Sonke*, et al.*, Recurrent inference machines for reconstructing heterogeneous MRI data*. Medical Image Analysis,* 2019. 53: p. 64-78.
7. Yousefi S., Hirschler L., M.C.E. Van der Plas*, et al.*, Fast Dynamic Perfusion and Angiography Reconstruction Using an End-to-End 3D Convolutional Neural Network. *In: Knoll F., Maier A., Rueckert D., Ye J. (eds) Machine Learning for Medical Image Reconstruction. MLMIR 2019. Lecture Notes in Computer Science, vol 11905. Springer, Cham. ,* 2019.
8. L. Zhao, S.W. Fielden, X. Feng*, et al.*, Rapid 3D dynamic arterial spin labeling with a sparse model-based image reconstruction*. NeuroImage,* 2015. 121: p. 205-216.
9. Y. Suzuki, T.W. Okell, M.A. Chappell and M.J.P. van Osch, A framework for motion correction of background suppressed arterial spin labeling perfusion images acquired with simultaneous multi-slice EPI*. Magn Reson Med,* 2019. 81(3): p. 1553-1565.
10. N.N. Graedel, J.A. McNab, M. Chiew and K.L. Miller, Motion correction for functional MRI with three-dimensional hybrid radial-Cartesian EPI*. Magn Reson Med,* 2017. 78(2): p. 527-540.

11. K. Nehrke and P. Bornert, Prospective correction of affine motion for arbitrary MR sequences on a clinical scanner. *Magn Reson Med,* 2005. 54(5): p. 1130-8.
12. R.W. Chan, E.A. Ramsay, C.H. Cunningham and D.B. Plewes, Temporal stability of adaptive 3D radial MRI using multidimensional golden means. *Magn Reson Med,* 2009. 61(2): p. 354-63.
13. J.G. Pipe, N.R. Zwart, E.A. Aboussouan*, et al.*, A new design and rationale for 3D orthogonally oversampled k-space trajectories. *Magn Reson Med,* 2011. 66(5): p. 1303-11.
14. W. Dai, P.M. Robson, A. Shankaranarayanan and D.C. Alsop, Reduced resolution transit delay prescan for quantitative continuous arterial spin labeling perfusion imaging. *Magn Reson Med,* 2012. 67(5): p. 1252-65.
15. M.J. van Osch, W.M. Teeuwisse, Z. Chen*, et al.*, Advances in arterial spin labelling MRI methods for measuring perfusion and collateral flow. *J Cereb Blood Flow Metab,* 2018. 38(9): p. 1461-1480.